

A NON-CLASSICAL RIEMANN PROBLEM FOR PIG MOTION IN ISOTHERMAL GAS PIPELINES

Simone Rodrigues de Melo, e-mail: simonermelo@gmail.com

Felipe Bastos de Freitas Rachid, e-mail: rachid@vm.uff.br

Laboratory of Liquid & Gas Transport - Francisco Eduardo Mourão Saboya Post-graduate Program of Mechanical Engineering (PG-MEC) - Department of Mechanical Engineering (TEM) - Universidade Federal Fluminense, Niterói, RJ, Brazil.

Abstract. *This paper presents the formulation along with its analytical solution of a non-classical Riemann problem for pig motion in transient isothermal gas pipelines. The pig motion modeling takes into account the existence of flow rate by-pass through its gap as well as through its body. Coulomb type as well as hydrodynamic friction forces are accounted for at the pig-pipe lateral interface. The proposed formulation is suitable for using with numerical methods based on the Riemann problem solution, such as Godunov, Glimm and MUSCL-Hancock schemes. Numerical solutions for the non-classical Riemann problem are presented for start-up the pig inside the line, for pigs with and without by-pass flow rates.*

Keywords: *Pig motion, gas pipelines, Riemann problem, non-classical Riemann problem*

1. INTRODUCTION

Pigs are commonly used in pipeline industry during not only commissioning but also different stages of operation to perform functions such as dewatering, cleaning and application of protective coatings. They are also used as key elements to separate different products (or different grades of a same product) batches through a same pipeline. Pigs are also routinely used to inspect pipelines for corrosion, internal damage, wall thickness, metal loss, pipe roundness, internal surface condition, cracks, etc. (Botros and Golshan , 2009).

Pigging operations are carried out not only in liquid and gas pipelines but also in two-phase gas pipelines. Due to its rather complex nature, the theoretical modeling of pig motion, along with a complete numerical solution coupled with the hydrodynamic equations governing the fluid flow in the pipeline, both in single-phase as well as in two-phase pipelines, is far from being a well-resolved issue. As a result, it has been the subject of intensive research in past years (Niecke et al. , 2001; Esmailzadeh et al. , 2009; Botros and Golshan , 2009; Bueno et al. , 2012).

The existing works dealing with the modeling of pig motion in pipelines and the numerical solution of the coupled pig motion and fluid flow are basically divided between single-phase (Azevedo et al. , 1997; Campo Barba and Freitas Rachid , 1997; Nguyen et al. , 2001; Esmailzadeh et al. , 2009; Botros and Golshan , 2009) and two-phase approaches (Kohda et al., 1988; Minami and Shoham , 1994; Xu X. and Gong , 2005; Bueno et al. , 2012). Since the pig lengths are significantly shorter than the pipeline extensions, the pig is always treated and modeled as being a singular surface in the cross-sectional area of the fluid flow. The difference among the models relies basically on the way the mechanical and hydrodynamic contact forces between the pig and the pipe wall are described, as well as the possibility or not to incorporate by-pass flow rates through the body of the pig and through the pig-pipe interface.

Two approaches have been used concerning the numerical procedures for obtaining approximating solutions to the resulting initial-boundary-value problem coupling the pig motion and unsteady flow. In the first one, the pig is effectively treated as a moving boundary, so that moving or adaptive grids are used at the left and at the right of the pig where boundary conditions are imposed. In the second approach, fixed grids are used and the dynamic equations for the pig are solved together with the fluid flow equations for a specific cell. For single-phase as well as for two-phase models, there is a widespread tendency to numerically solve the pig motion and fluid flow coupled problems by using finite difference

schemes. For single-phase flows, the method of characteristics is the most commonly used technique (Campo Barba and Freitas Rachid, 1997; Nguyen et al., 2001; Esmailzadeh et al., 2009; Botros and Golshan, 2009).

On the other hand, it is well-known that finite difference schemes are not capable to deal with, and also keep track of, strong discontinuities in the solution. The method of characteristics does not work properly whenever the wavefront speeds vary significantly from one point to another inside the domain. These shortcomings introduce non-realistic dispersion and attenuation in the numerical solution, what can compromise their applications to these specific problems.

As an alternative to the aforementioned numerical techniques, it is proposed in this paper a non-classical Riemann problem for the pig motion problem in single-phase flows, along with a complete numerical strategy for obtaining an approximating solution. The proposed formulation is suitable for using with numerical methods based on the Riemann problem solution, such as Godunov, Glimm, MUSCL-Hancock schemes and others. These methods are recognized as one of those that better captures and preserves the presence of discontinuities in the dependent variables and their derivatives (Toro, 1999).

2. GOVERNING EQUATIONS

Since the pipeline diameter D is such that, $D \ll L$, in which L stands for the pipeline extension, pressure transients in isothermal gas pipelines are commonly described by means of one-dimensional models. Moreover, since $L_p \ll L$, in which L_p stands for the pig length, the pig is usually considered a singular surface or more precisely a singularity in the one-dimensional context. Thus, by assuming that the pipe wall is rigid and that $x_p = x_p(t)$ represents the pig position in the current time instant t , the governing equations describing the pig movement in isothermal gas pipelines can be written in Eulerian coordinates in the following canonical form of conservation laws:

$$\partial_t \mathbf{u} + \partial_x \mathbf{F}(\mathbf{u}) = \mathbf{S}(\mathbf{u}) \quad \text{in} \quad (0, x_p) \cup (x_p, L) \times (0, \infty) \quad (1)$$

in which $\mathbf{u}(x, t) = \mathbf{u} \in \mathbb{R}^2$ is the conserved quantity, x is the spatial coordinate along the pipe centerline and t is the time instant. The symbols $\partial_t \chi$ and $\partial_x \chi$ are used to designate partial derivative of a general dependent variable χ with respect to t and x , respectively. The vector-valued functions $\mathbf{F}(\mathbf{u}) = \mathbf{F} : \mathbb{R}^2 \rightarrow \mathbb{R}^2$ and $\mathbf{S}(\mathbf{u}) = \mathbf{S} : \mathbb{R}^2 \rightarrow \mathbb{R}^2$ are the flux and the source/sink terms, respectively. The particular form of these vector quantities are:

$$\mathbf{u} := (u_1, u_2)^T := (\rho, \rho v)^T \quad (2)$$

$$\mathbf{F} := (u_2, u_2^2/u_1 + p)^T \quad (3)$$

$$\mathbf{S} := (0, -u_1 g \sin \theta - (u_1 f(u_2/u_1) |(u_2/u_1)|) / (2D))^T \quad (4)$$

in which $p := a^2 \rho$. In the above equations, which represent the balances of mass and momentum for the gas within the pipeline, p and v are functions of the time t and the spatial position x along the pipe and represent, respectively, the pressure and the axial gas velocity. The angle formed between the pipe centerline and the horizontal is designated by θ , whereas g and f stand for the local gravitational acceleration and the Darcy-Weisbach friction factor. The term a stands for the isothermal wave speed in the gas and is treated herein as a positive constant.

The governing equations are completed by adding the balance of momentum for the pig and the balance equation of mass for the gas through it, along with some constitutive equations for the by-pass flow rate. By denoting p^- and p^+ as being the pressures behind and ahead of the pig, the balance of linear momentum for the pig can be written as follows:

$$M_p \frac{dv_p}{dt} = (p^- - p^+) A - M_p g \sin \beta - F_H - F_M, \quad (5)$$

in which $A = \pi D^2/4$ is the cross-sectional area of the pipe, M_p stands for the mass of the pig and v_p its velocity, i.e.; $dx_p/dt = v_p$. The first term on the right-hand side of Eq.(5) represents the driving force and the second one the component of the pig weight in the direction of the motion. The third and fourth terms on the right-hand side represent the hydrody-

dynamic and mechanical friction forces, acting on the nominal lateral contact surface, whose area is A_c ($A_c = \pi DL_p$). By admitting an idealized mean gap width between the pig and the pipe, the existence of a fluid flow through this gap will induce one resistive hydrodynamic force acting on the pig lateral contact surface. Under the assumptions of fully-developed flow of a Newtonian incompressible fluid, this force derived by (Azevedo et al. , 1997) can be expressed by:

$$\bar{F}_H = A_c \left(\mu \frac{\nu_p}{\delta} - \frac{(p^- - p^+)}{2L_p} \delta \right), \quad (6)$$

in which μ stands for the absolute viscosity of the gas.

On the other hand, by admitting that the idealized pig is a solid cylindrical dowel of radius r_p , with an oversize $\Delta r = r_p - D/2$, and is submitted to the pressure loadings p^- and p^+ on their opposite surfaces, a Coulomb-like mechanical friction force will develop at the pig lateral contact surface. Under the assumptions of the infinitesimal elasticity theory, this contact force may be approximated by (Gomes , 1994):

$$\bar{F}_M^{(l)} = A_c \eta_l \frac{1}{1 - \nu} \left(\frac{E \Delta r}{r_p} + \nu \frac{(p^- + p^+)}{2} \right), \quad (7)$$

in which E and ν are the equivalent Young modulus and Poisson ratio of the idealized pig, whereas η_l , with $l \in \{s, d\}$, stands for the static ($l = s$) or dynamic ($l = d$) friction coefficient, with $\eta_s > \eta_d$. Since the hydrodynamic and mechanical forces most likely act simultaneously in complementary areas of the total area of the lateral surface, it is convenient to introduce the concept of dry contact area ratio define as:

$$\xi = \frac{A_M}{A_c}, \quad (8)$$

in which A_M represents the dry area in which the mechanical force acts and $\xi \in [0, 1]$. The dry contact area ratio can or cannot be assumed as being constant throughout the pig motion, according to the type of pig. For the sake of completeness, it could be expressed as being a function of the pig velocity, i.e., $\xi = \hat{\xi}(\nu_p)$. Taking into account Eq.(8), the hydrodynamic force can be written as

$$F_H = (1 - \xi) \bar{F}_H, \quad (9)$$

and the mechanical force expressed in terms of the prevailing condition of the pig motion (Campo Barba and Freitas Rachid , 1997) according to:

$$F_M = \begin{cases} \text{sgn}(v_p) \xi \bar{F}_M^{(d)}, & \text{if } v_p \neq 0; \\ \text{sgn}(F^*) \xi \bar{F}_M^{(s)}, & \text{if } v_p = 0 \text{ and } dv_p/dt \neq 0; \\ F^*, & \text{if } v_p = 0 \text{ and } dv_p/dt = 0; \end{cases} \quad (10)$$

in which $F^* = (p^- - p^+) A - F_H - M_p g \sin \beta$.

To complete the physical description of the interaction of the pig motion along with the gas flow, it remains to ensure that the continuity principle is satisfied through the pig. In the context of the modeling presented so far, it is done by applying the balance of mass for the singular surface at the pig position. By denoting ρ^-, u^- and ρ^+, u^+ , the mass densities and velocities at the left and at the right of the pig, it comes out that:

$$\rho^- A (v^- - v_p) = \rho^+ A (v^+ - v_p) = \dot{m}. \quad (11)$$

Equation (11) states that the mass flow rate of gas transposing the pig must be equal when computed at the left and at the right of it. Moreover, this mass flow rate is the total by-pass mass flow rate for which a constitutive relationship must be provided. By assuming that the total by-pass flow rate comes from the contribution of three distinct parcels through:

the gap $\bar{\rho}Q_g$, the holes in the pig body $\bar{\rho}Q_h$ and its permeable body $\bar{\rho}Q_b$ then:

$$\dot{m} = \bar{\rho}(I_g Q_g + I_h Q_h + I_b Q_b), \quad (12)$$

in which $\bar{\rho} = \sqrt{\rho^+ \rho^-}$, with I_g , I_h and I_b assuming either 0 or 1, according to the existence or not of this specific by-pass flow rate type. Under proper simplifying assumptions, (Azevedo et al. , 1997) has demonstrated that the by-pass volumetric flow rate can be expressed by:

$$Q_g = \pi D \left(\frac{\delta^3}{12\mu} \frac{(p^- - p^+)}{L_p} - \frac{\delta}{2} v_p \right). \quad (13)$$

Under the assumption that the flow through a hole in the pig does not disturb the flow through the others, one possible approximation for this volumetric by-pass flow rate is:

$$Q_h = \text{sgn}(p^- - p^+) \frac{n\pi d^2}{4} \sqrt{\frac{2|p^- - p^+|/\bar{\rho}}{k_h}}, \quad (14)$$

in which n represents the numbers of holes, whose diameter is d and head loss coefficient is k_h . Finally, if the pig body is a permeable porous media, then the volumetric flow rate can be approximated by using the Darcy's law:

$$Q_b = \frac{\pi D^2 K}{4\mu} \frac{(p^- - p^+)}{L_p}, \quad (15)$$

in which K stands for the permeability of the pig body with respect to the gas.

Equations (1) along with Eqs. (5), (11) and (12) form a complete set of non-linear hyperbolic differential equations with a moving boundary $x_p(t) \in (0, L)$. These equations involves the unknowns p and v in $(0, x_p) \cup (x_p, L)$ and v_p , along with p^- , p^+ , v^- and v^+ at the left and at the right of the pig.

3. THE ASSOCIATED NON-CLASSICAL RIEMANN PROBLEM AND ITS SOLUTION

The Riemann problem associated to the homogeneous (with $\mathbf{S}(\mathbf{u}) = \mathbf{0}$) system of equations (1) is an initial-value problem with discontinuous data at the left and at the right of an arbitrary position x_o , given at an arbitrary time instant t_o . For isothermal gas flows, its solution has been presented in several textbooks, see for instance (Toro , 1999), and worths for $t > t_o$ and every $x \in (-\infty, x_o) \cup (x_o, +\infty)$. The main purpose of this paper is to extend the formulation of the Riemann problem to cope with the presence of the pig in the line. To achieve this goal, instead of seeking a solution for $t > t_o$ as it is usually done in classical Riemann problems, we seek a solution within a time interval $t_o < t \leq t_f$, with t_f sufficiently close to t_o to ensure existence of the solution. Furthermore, we assume as a basic premise that the pig velocity remains constant and equal to $v_p(t_f)$ during this time interval. Thus, the non-classical Riemann problem for the pig, centered at $x_o = x_p(t_o)$, consists in to find $\mathbf{u}(x, t)$, $v_p(t_f)$, p^- , v^- , p^+ and v^+ via,

$$\partial_t \mathbf{u} + \partial_x \mathbf{F}(\mathbf{u}) = \mathbf{0} \quad \text{in} \quad (-\infty, x_p(t_o)) \cup (x_p(t_o), +\infty) \times (t_o, t_f), \quad (16)$$

subjected to the following discontinuous initial data:

$$\mathbf{u}(x, t) = \begin{cases} \mathbf{u}_L = (p_L, v_L)^T, & \text{for } x < x_p(t_o); \\ \mathbf{u}_R = (p_R, v_R)^T, & \text{for } x > x_p(t_o); \end{cases} \quad (17)$$

in which \mathbf{u}_L and \mathbf{u}_R are arbitrary and constant states, along with Eqs. (5), (11) and (12).

Within the context of the non-classical Riemann problem, the pig acceleration remains constant in the time interval $(t_o, t_f]$ what implies that the variables p^- , v^- , p^+ and v^+ also remain constant. As a consequence, the problem given by

Eqs. (16) and (17), along with Eqs. (5), (11) and (12) is invariant under the scale transformation $x' = \alpha(x - x_p(t_o))$ and $t' = \alpha(t - t_o)$, with $\alpha > 0$, and its solution depends only on the ratio $\xi = (x - x_p(t_o))/(t - t_o)$. In other words, it is of the form $\tilde{\mathbf{u}}(x, t) = \hat{\mathbf{u}}(\xi)$, for $t_o < t \leq t_f$, where $\hat{\mathbf{u}} : \mathbb{R} \rightarrow \mathbb{R}^2$ is a piecewise continuous function.

It can be shown that the (generalized) solution of this particular problem is constructed by connecting the left state \mathbf{u}_L to the right state \mathbf{u}_R through intermediate states \mathbf{u}_L^* and \mathbf{u}_R^* which should be determined. Since the pig is a contact discontinuity (c.d.) which travels with a constant speed $v_p(t_f)$ and, from the eigenstructure of Eq. (16), there are two eigenvalues $\lambda_1 = v - a$ and $\lambda_2 = v + a$ to which a 1-wave and a 2-wave are associated with, then by assuming that $\lambda_1 < v_p < \lambda_2$ and that $v/a < 1$ the (generalized) solution of this problem is constructed by connecting the aforementioned states in the following manner: $\mathbf{u}_L \xrightarrow{1\text{-wave}} \mathbf{u}_L^* \xrightarrow{\text{pig c.d.}} \mathbf{u}_R^* \xrightarrow{2\text{-wave}} \mathbf{u}_R$. The 1-wave and the 2-wave may be either rarefactions or shocks, according to the conditions at the left and at the right (Toro, 1999). By defining $M_L(p_L^*)$ and $M_R(p_R^*)$ as indicated below, it can be shown that:

$$M_L(p_L^*) := \frac{p_L^* - p_L}{v_L - v_L^*} = \frac{p_L}{a} \phi\left(\frac{p_L^*}{p_L}\right) \quad \text{for 1-wave} \quad (18)$$

$$M_R(p_R^*) := \frac{p_R^* - p_R}{v_R^* - v_R} = \frac{p_R}{a} \phi\left(\frac{p_R^*}{p_R}\right) \quad \text{for 2-wave} \quad (19)$$

in which,

$$\phi(z) = \begin{cases} \frac{z-1}{\ln z}, & \text{if } z < 1 \text{ (rarefactions)} \\ \sqrt{z}, & \text{if } z \geq 1 \text{ (shocks)} \end{cases} \quad (20)$$

By noting that $p^- = p_L^*$, $p^+ = p_R^*$, $v^- = v_L^*$ and $v^+ = v_R^*$, Eqs. (11), (18) and (19) can be combined to form, along with Eq. (5), the following system of differential and algebraic equations in terms of v_p and $\mathbf{y} = (p_L^*, p_R^*)^T$:

$$\frac{dv_p}{dt} = \frac{1}{M_p} ((p_L^* - p_R^*) A - M_p g \sin \beta - F_H - F_M) \quad (21)$$

$$\mathbf{g}(v_p, \mathbf{y}) = \mathbf{0}, \quad (22)$$

in which

$$g_1 = p_L^* - p_L - M_L(p_L^*) \left(v_L - \frac{\dot{m} a^2}{A p_L^*} - v_p \right) \quad (23)$$

$$g_2 = p_R^* - p_R - M_R(p_R^*) \left(\frac{\dot{m} a^2}{A p_R^*} + v_p - v_R \right) \quad (24)$$

with $\dot{m} = \hat{m}(p_L^*, p_R^*, v_p)$. The solution at $t = t_f$ of the system of Eqs. (21-22), which is carried out by using the Petzold-Gear BDF method (Petzold, 1982), completes the solution of the non-classical Riemann problem for the pig.

4. NUMERICAL SIMULATIONS

In order to evaluate the capability of the proposed non-classic Riemann problem, along with its numerical solution, in properly dealing with the pig movement problem, we present next some numerical results for typical cases involving the pig motion in gas pipelines. Since the critical cases involving pig motion are those associated with its start-up, we take this physical situation as the main motivation in the numerical simulations presented ahead.

The pig is assumed to be at rest ($v_p(t = t_o = 0) = 0$) inside a long and horizontal ($\theta = 0.0$) gas pipeline, whose internal diameter is $D = 0.6096$ m. At room temperature, the isothermal wave speed of the gas is $a = 414$ m/s and its absolute viscosity is equal to $\mu = 1.5 \times 10^{-5}$ Pa.s. The physical properties of the pig are: $r_p = 0.30988$ m, $M_p = 200$ kg, $E = 36.16$ MPa, $\nu = 0.15$, $L_p = 0.2$ m, $\eta_s = 0.25$, $\eta_d = 0.23$.

To assess the robustness of the proposed strategy in dealing with different real-world situations, three different cases,

hereto after labeled as Case A, B and C, were considered with regard to the by-pass flow through the pig. In Case A, an idealized situation is considered in which there is no by-pass flow at all. This situation is mimic by assuming that there is no gap between the pig and the pipe ($\delta = 0.0$) and, as a consequence, the contact area ratio is equal to $\xi = 1.0$ and so no hydrodynamic force acts on the lateral contact area of the pig. In Case B it is assumed that the by-pass flow takes place solely through the gap, which is of the order of $\delta = 0.1$ mm. Finally, in Case C, besides the by-pass flow through the gap, there exists also a parcel of by-pass flow through four holes ($n_h = 4$) in the pig's body, having each one a head loss coefficient equal to $k_h = 3.0$. The physical features of these three cases are shown in Table 1, where it can be seen that a same contact area ratio of $\xi = 0.8$ has been adopted for both Cases B and C.

Table 1. Description of the non-classical Riemann problems for the three cases.

Case	Description	δ (mm)	ξ (-)	n_h (-)	k_h (-)
A	no by-pass flow	0.0	1.0	0.0	0.0
B	by-pass through the gap only	0.1	0.8	0.0	0.0
C	by-pass through the gap and holes in the pig's body	0.1	0.8	4.0	3.0

The initial data of the non-classical Riemann problem concerning the pressures and velocities of the gas ahead (p_L, v_L) and behind the pig (p_R, v_R) (see Eq. 17) are presented in Table 2 for the three cases A, B and C. These data were chosen by following a two-step procedure. Firstly, by fixing the pressure behind the pig p_R , Eqs. (21-22) were solved with $v_p = 0$ and $dv_p/dt = 0$ to find the corresponding equilibrium values v_L, v_R and p'_L . In the sequel, p_L was computed by setting $p_L = p'_L + \Delta p$, in which $\Delta p = N \sqrt{\rho_L \rho_R} a v_{ref}$, with v_{ref} being the velocity reference of the gas inside the pipeline. The value of Δp is an increase in the pressure ahead of the pig to set it in motion and represents N times the Joukowski pressure surge. In constructing Table 2, we have used $v_{ref} = 9$ m/s and $N = 3$, in such a way that $p_L - p_R$ represents a severe pressure gradient mimicking stringent situations of pig start-up.

Table 2. Initial data of the non-classical Riemann problems for the three cases.

Initial data	Case A	Case B	Case C
(p_L, p_R) (Pa)	(4884073, 4210703)	(4884657, 4210703)	(4884656, 4210703)
(v_L, v_R) (m/s)	(0, 0)	(0.0675, 0.07371)	(0.7337, 0.8012)

The results of the numerical simulations associated with the solution of the non-classical Riemann problem, with initial data given in Table 2, are depicted in the graphs of Figs. 1, 2 and 3 for the Cases A, B and C, respectively. To evaluate the robustness of the numerical strategy, these solutions were obtained for the maximum value of $t_f, [t_f]_{max}$, for which a numerical solution was feasible, i. e., for $t_f > [t_f]_{max}$ convergence to a numerical solution was not achieved. The values of $[t_f]_{max}$ for each of the Cases A, B and C are presented in Table 3.

Table 3. Reference values for plotting purpose for the three cases.

Reference values	Case A	Case B	Case C
$[t_f]_{max}$ (s)	0.1	0.008	0.001
p_{max} (Pa)	4884073	4884657	4884657
v_{max} (m/s)	9.69	3.32	1.53

For uniformly plotting the results allowing to establish comparisons among them, the pressure, the velocity, the time and the spatial position are scaled according to:

$$P := \frac{p}{p_{max}} \quad ; \quad V := \frac{v}{v_{max}} \quad ; \quad T := \frac{t}{[t_f]_{max}} \quad ; \quad X := \frac{x}{L} \quad ; \quad (25)$$

in which $L = 100$ m and the maximum values of velocity and pressure for each case were computed as follows:

$$v_{max} = \max [|v_L|, |v_R|, |v_L^*|, |v_R^*|] \quad (26)$$

$$p_{max} = \max [|p_L|, |p_R|, |p_L^*|, |p_R^*|, \max [\rho_L, \rho_R, \rho_L^*, \rho_R^*] v_{max} a]. \quad (27)$$

The values of v_{max} and p_{max} for the three Cases A, B and C are also presented in Table 3.

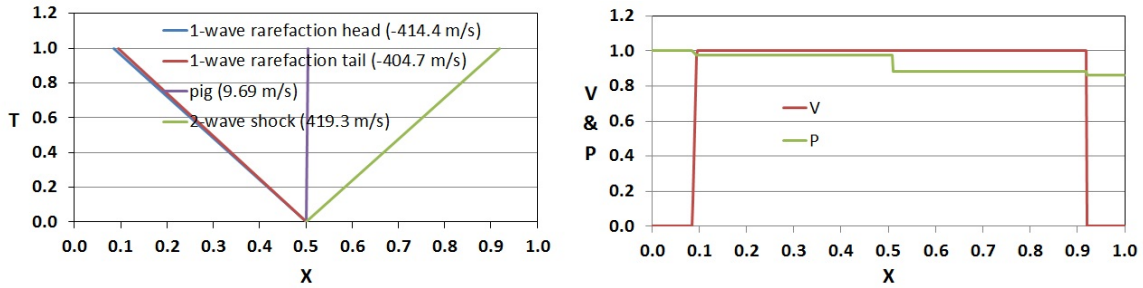


Figure 1. Solution representation of the non-classical Riemann problem for Case A in the T - X plane (left) and for the V and P variables against X (right) at time $T = 1$.

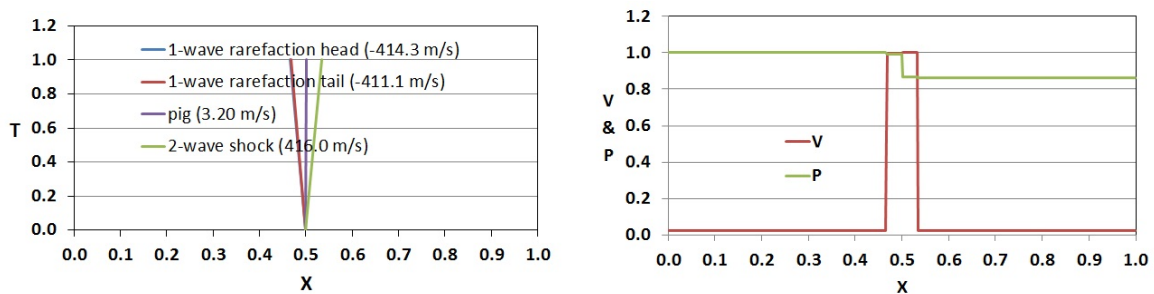


Figure 2. Solution representation of the non-classical Riemann problem for Case B in the T - X plane (left) and for the V and P variables against X (right) at time $T = 1$.

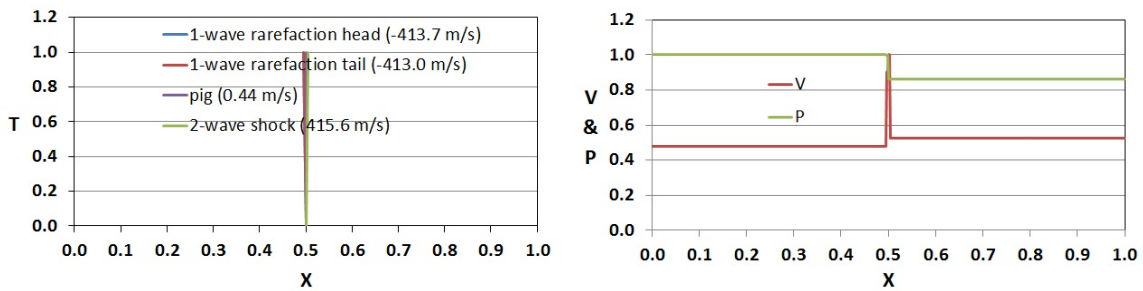


Figure 3. Solution representation of the non-classical Riemann problem for Case C in the T - X plane (left) and for the V and P variables against X (right) at time $T = 1$.

Independently of the existence and quantity of the by-pass flow rate, it can be observed in the left graphs of Figs. 1, 2 and 3 that the solution of the pig start-up described by the non-classical Riemann problem for Cases A, B and C is always of the same nature, i. e., 1-rarefaction/2-shock. However, it can be seen in Table 3 that as the amount of by-pass flow rate is increased from Case A to Case C, the numerical solution of the problem is achieved for decreasing values of $[t_f]_{max}$, what explains the relative positions of these waves compared to the pig contact discontinuity in the X - T planes of the left graphs of Figs. 1, 2 and 3.

Although small time-steps are required to ensure the existence of a numerical solution of the non-classical Riemann problem when the by-pass flow rate through the pig increases, a numerical solution seems always to exist even in these most critical situations associated with pig start-up.

5. CONCLUDING REMARKS

A non-classical Riemann problem, along with its solution and a numerical strategy for computing it, has been proposed in this paper for analyzing pig motion in gas pipelines during unsteady and steady states. Numerical solutions have then been carried out for the practical problem associated with the pig start-up. Different situations ranging from no by-pass flow to by-pass flow through the gap and through the holes in the pig's body are considered. The results obtained have shown that a numerical solutions always exist, but small time-steps are required to advance the solution in time when the by-pass flow rate through the pig increases.

6. ACKNOWLEDGEMENTS

The authors would like to thank Petrobras S.A., CNPq, CAPES and FAPERJ for the continuous support of all research activities of this group over the years. The first author also gratefully acknowledges the scholarship granted by the CAPES agency during the M.Sc. course in the PGMEC at Universidade Federal Fluminense.

7. REFERENCES

- Azevedo L. F. A, Braga A.M.B. and Gomes M.G.F.M., 1997. "Experimental validation of analytical models for by-pass flow and contact forces in pig cups". In *Proceedings of the Pipeline Pigging Conference*. Houston, Texas, USA.
- Botros K.K. and Golshan H., 2009. "Dynamics of pig motion in gas pipelines". In *Proceedings of the AGA Operations Conference & Biennial Exhibition*. Pittsburgh, USA. May, pp. 19–21.
- Bueno, D. E. G. P., Figueiredo, A. B., Baptista, R. M., Freitas Rachid, F. B. and Bodstein, G. C. R., 2012. "Featuring pig movement in two-phase gas pipelines". In *Proceedings of the 9th International Pipeline Conference*, pp. 1–10, Calgary, Alberta, Canada.
- Campo Barba, E.V. and Freitas Rachid, F.B., "Modeling of pig motion under transient fluid flow". In *Proceedings of the XIV Brazilian Congress of Mechanical Engineering COBEM*. São Paulo, Brazil.
- Esmailzadeh, F., D. Mowla D. and Asemani M., 2009. "Mathematical modeling and simulation of pigging operation in gas and liquid pipelines". *Journal of Petroleum Science and Engineering*, Vol. 69, pp. 100–106.
- Gomes, M. G. F. M., 1994. *The analysis cup pigs by the finite element method*. M.Sc. Thesis, Federal University of Rio de Janeiro, Rio de Janeiro, Brazil.
- Kohda, K., Suzukawa, Y. and Furukawa, H., 1988. "Pigging analysis for gas-liquid two-phase flow in pipelines". In *Proceedings of the 11th Annual Energy Resources Technology Conference & Exhibition*. New Orleans, USA.
- Minami, K. and Shoham, O., 1994. "Transient two-phase flow behavior in pipelines - Experiment and modeling". *International Journal of Multiphase Flow*, Vol. 20, pp. 739–752.
- Nieckele, A.O., Braga, A.M.B. and Azevedo, L.F.A., 2001. "Transient pig motion through gas and liquid pipelines". *Journal of Energy Resources Technology*, Vol. 123, pp. 260–269.
- Nguyen, T.T., Yoo, H.R., Rho, Y.W. and Kim S.B., 2001. "Modeling and simulation for pig with bypass flow control in natural gas pipeline". *KSME International Journal*, Vol. 15, pp. 1302–1310.
- Petzold, L.R., 1982. "A description of DASSL: A differential-algebraic system solver". In *Proceedings of the IMACS World Congress*, Montreal, Canada.
- Toro, E.F., 1999. *Riemann solvers and numerical methods for fluid dynamics*. Springer.
- Xu, X. and Gong, J., 2005. "Pigging simulation for horizontal gas-condensate pipelines with low-liquid loading". *Journal of Petroleum Science and Engineering*, Vol. 48, pp. 272–280.

8. RESPONSIBILITY NOTICE

The author(s) is (are) the only responsible for the printed material included in this paper.